JOURNAL OF GEOPHYSICAL RESEARCH, VOL. 104, NO. D2, PAGES 2059–2066, JANUARY 27, 1999

Absorption of solar radiation by the cloudy atmosphere: Further interpretations of collocated aircraft measurements

Robert D. Cess,[1] Minghua Zhang,[1] Francisco P. J. Valero,[2] Shelly K. Pope,[2] Anthony Bucholtz,[2] Brett Bush,[2] Charles S. Zender,[3] and John Vitko Jr.[4]

Abstract. We have extended the interpretations made in two prior studies of the aircraft shortwave radiation measurements that were obtained as part of the Atmospheric Radiation Measurements (ARM) Enhanced Shortwave Experiment (ARESE). These extended interpretations use the 500 nm (10 nm bandwidth) measurements to minimize sampling errors in the broadband measurements. It is indicated that the clouds present during this experiment absorb more shortwave radiation than predicted by clear skies and thus by theoretical models, that at least some ($\leq$20%) of this enhanced cloud absorption occurs at wavelengths $<$680 nm, and that the observed cloud absorption does not appear to be an artifact of sampling errors nor of instrument calibration errors.

1. Introduction

The U.S. Department of Energy, as part of its Atmospheric Radiation Measurements (ARM) Program, organized the ARM Enhanced Shortwave Experiment (ARESE), which was held in fall 1995. Full descriptions of ARESE and the rationale for performing it are provided by *Valero et al*. [1997a, b] and *Zender et al*. [1997]. Briefly stated, the purpose of ARESE was to address the issue of cloud shortwave (SW) absorption. Do clouds, as suggested by several recent studies, absorb more SW radiation than predicted by theoretical models? And, because theoretical models predict roughly the same SW absorption for clear and cloudy conditions, then do cloudy skies absorb significantly more SW radiation than do clear skies? Or, as suggested by others, is this observed excess SW absorption actually the consequence of sampling errors or instrument calibration errors?

Pertinent results from *Valero et al*. [1997b] are shown in Figure 1, based on radiometric measurements made from two collocated aircraft, an upper aircraft flying above the clouds at an altitude of roughly 14 km, and a lower aircraft flying below the clouds at altitudes ranging from 0.5 to 2 km. The absorptances shown in Figure 1 represent the fraction of the downwelling SW radiation (insolation) measured at the upper aircraft altitude that is absorbed by the atmospheric column located between the two aircraft; i.e., they denote the SW absorption within the atmospheric column normalized by the insolation as measured at the upper aircraft. The broadband absorptance refers to the spectral interval from 225 to 3910 nm, while the 500 nm absorptance refers to a 10 nm bandwidth centered at 500 nm. These absorptances have been recalculated using slightly revised data released on September 3 and 5, 1997. The differences from *Valero et al*. [1997b], however, are insignificant. The error bars in Figure 1 were computed using a 1% relative instrument precision [*Valero et al*., 1977b], adopting the extreme assumption that the instrument errors are additive. Figure 1 refers to flight-time averages for 4 days spanning increasing cloudiness (left to right) from clear skies on October 11, 1995, to heavy overcast conditions on October 30, 1995. The point of Figure 1 is that as cloudiness increases, the broadband absorptance increases significantly relative to that for clear skies (October 11), consistent with several studies, as summarized by *Valero et al*. [1997b], that suggest clouds absorb more SW radiation than observed for clear skies and consequently, as predicted by theoretical models.

The purpose of the present study is to extend the interpretations of the ARESE aircraft measurements by *Valero et al*. [1997b] with three specific goals.

1. We wish to provide a plausible explanation for the magnitude of the 500 nm absorptances shown in Figure 1. This is important because the 500 nm absorptance plays a crucial role in understanding sampling errors, as elucidated by *Valero et al*. [1997a, b] and as will additionally be demonstrated in this study, and their magnitude ($\approx$0.05) is considerably in excess of that caused by ozone, which is the only known gaseous absorber at 500 nm.
2. Because of its importance and its historic confusion, the issue of sampling errors will be revisited. Specifically, it will be demonstrated that the enhanced cloud absorption evidenced in Figure 1 is unlikely to be an artifact of sampling errors.
3. There have been suggestions that instrument calibration errors might be the cause of the enhanced cloud absorption shown in Figure 1, and it will be demonstrated that such errors are likewise unlikely.

2. The 500 nm Absorptance

We address the issue of the 500 nm absorptances by considering a subset of the aircraft measurements made on October 11 under cloud-free conditions. Illustrated in Figure 2a are the upper aircraft and lower aircraft altitudes (1-s means) throughout the flight on that day. The small data gaps are the result of the top speed of the lower aircraft being below the upper aircraft's slowest operational speed, so that the upper aircraft had to periodically perform 360° turns, after which it would be behind the lower aircraft and then proceed past the lower

[1]Marine Sciences Research Center, State University of New York, Stony Brook.
[2]Scripps Institution of Oceanography, University of California at San Diego, La Jolla.
[3]National Center for Atmospheric Research, Boulder, Colorado.
[4]Sandia National Laboratory, Livermore, California.

Paper number 1998JD200058.
0148-0227/99/1998JD200058$09.00

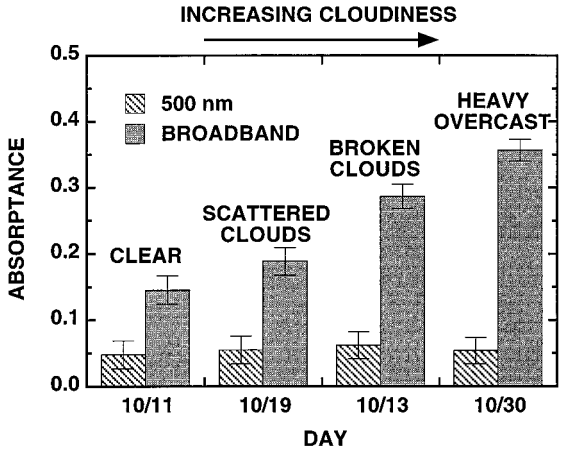

Figure 1. The column band absorptance as determined from broadband (224–3910 nm) and total, direct, diffuse radiometer (10 nm spectral bandwidth centered at 500 nm) measurements for each of the 4 days, progressing from clear skies on the left to heavy overcast conditions on the right.

aircraft, subsequently performing another turn. Data taken during the turns were deleted for both aircraft. The larger gaps represent periods when the lower aircraft was changing altitude, or both aircraft had reached the end of the flight path and thus both performed turns to proceed along the reverse flight path. Note the variability in lower aircraft altitude. The higher altitude at the initiation of the flight was to avoid the flight path of Vance Air Force Base, as was also the case at roughly 1620, after which the lower aircraft returned to and remained at the higher altitude as the result of turbulence.

Aside from aerosols, the only known clear-sky absorber at 500 nm is ozone, which by itself, cannot account for the large (≈0.05) 500 nm absorptance shown in Figure 1 for October 11. Water vapor exhibits no known absorption at 500 nm. Tropospheric aerosols constitute a likely candidate for this additional absorption, and because the abundance of tropospheric aerosols decreases with increasing altitude, we elected to concentrate on the latter portion of the October 11 flight, as indicated in Figure 2a, when the lower aircraft was flying a relatively constant and high altitude of roughly 1.7 km. The hope was that this high-altitude segment flown by the lower aircraft would minimize the concentration of tropospheric aerosols between the two aircraft. Figure 2b shows the flight path during this flight segment, and the final portion of the flight, denoted by the dotted line, appears to be in a nearly aerosol-free environment, as demonstrated by the 500 nm absorptance and transmittance results shown in Figure 2c. These consist of binned data of equal population, with the two pairs of absorptance and transmittance points on the right representing the final portion of the flight. Aerosol absorption should be insignificant during this flight portion, since the 500 nm absorptance is nearly zero and, as will be demonstrated, is consistent with ozone absorption. Because the aircraft are retracing their flight paths during this final flight portion, the low aerosol loading is probably the result of an air mass moving into the area rather than the aircraft moving into an aerosol-free environment. This is consistent with large wind speeds (6–12 m/s) between the altitudes of roughly 1 and 3 km as measured at the southwest end of the flight path at the time of the flight. An abrupt reduction in relative humidity could also cause a significant decrease in the radiative role of aerosols, but no such reduction was noted in profile measurements made at this location.

Aerosol variability within the atmospheric column is a plausible explanation for the changes in the 500 nm absorptance and transmittance values shown in Figure 2b because of the strong correlation between these two quantities as demonstrated in Figure 3a; a decrease in aerosol loading simultaneously decreases absorptance and increases transmittance. Moreover, the "clean air" points, at the lower corner of the plot, are consistent with small absorption by ozone and the absence of aerosols, as demonstrated by the model agreement shown in Figure 3a. The model used is that described by *Zender et al*. [1997], with the ozone profile taken from the ozone sondes at the site's Central Facility, an aerosol single scattering albedo of 0.83, and aerosol optical depths, progressing from right to left, of 0.00 (clean air), 0.06 and 0.12. Thus for this

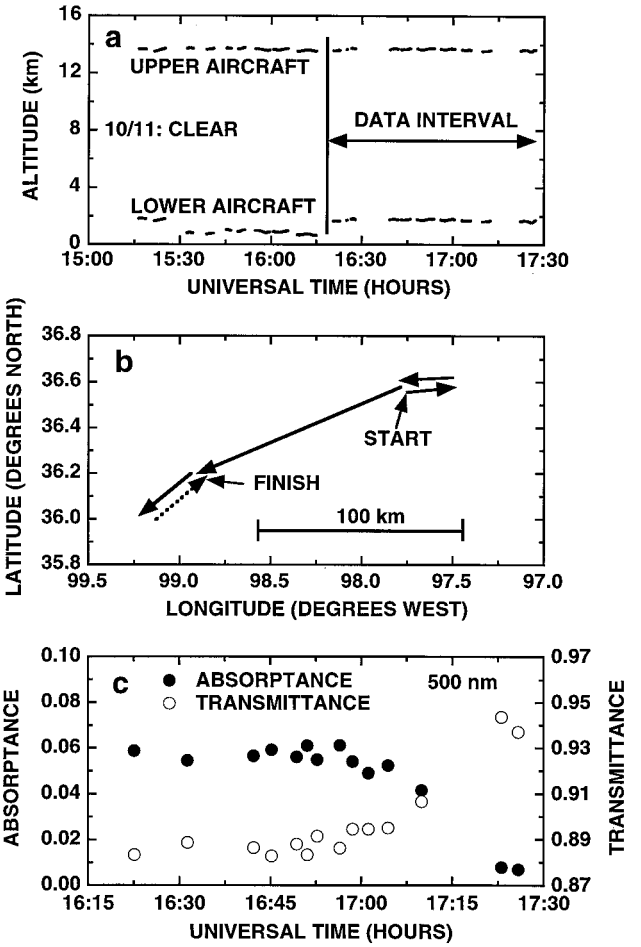

Figure 2. (a) The upper and lower aircraft altitudes as a function of universal time on October 11. These represent 1-s means. (b) The aircraft flight paths for the data interval shown in Figure 2a. The site's Central Facility is located at the start of the flight segment, and a boundary facility is located at the southwestern end of the segment. (c) The 500 nm column absorptance and transmittance, for the data interval shown in Figure 2a, as a function of universal time. These comprise equal-population binned data, with the two pairs of right-side points referring to the dotted portion of the flight path in Figure 2b.

aerosol model, Figure 2a suggests the maximum aerosol optical depth between the two aircraft was about 0.09, a value that is compatible with the total-atmosphere aerosol optical depth of 0.12 determined from surface measurements at the site's Central Facility at this time [*Zender et al*., 1997]. A less absorbing aerosol model will essentially retain the observed absorptance-transmittance slope, and this is demonstrated in Figure 3b for an aerosol single scattering albedo of 0.95. Alternatively, *Kato et al*. [1997, p. 25,881] suggest the presence of "some gaseous absorption process at visible wavelengths," and since the modeled absorptance-transmittance slope is relatively insensitive to the single scattering albedo (slope = -0.93 for $\omega = 0.95$ and slope = -1.11 for $\omega = 0$, as would be representative of gaseous absorption), the present data cannot realistically distinguish between aerosol and gaseous absorption. However, if a gas were the cause of the observed variability in Figure 3, it would require that the unknown gaseous absorber be temporally variable, and we regard this as a less likely candidate than aerosol variability, particularly since aerosols were known to be present on October 11 from surface measurements. Irrespective of the cause, however, the results shown in Figure 3 are consistent with the presence of a temporally variable absorber, which would explain the large (relative to ozone absorption) 500 nm absorptance shown in Figure 1 for October 11.

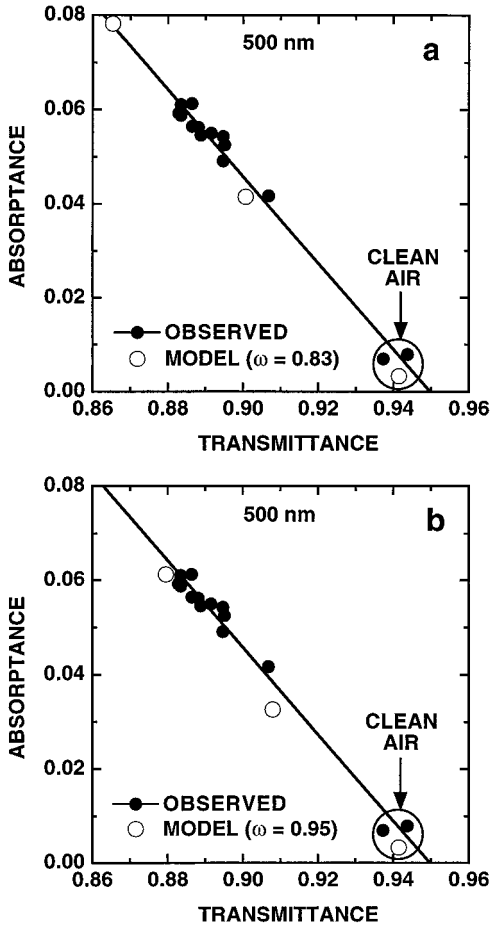

Figure 3. (a) The 500 nm absorptance versus 500 nm transmittance; these are the same binned data as in Figure 2c. The straight line is a linear fit to the data. Also shown are modeled absorptance and transmittance values for an aerosol single scattering albedo (ω) of 0.83 and for aerosol optical depths, progressing from right to left, of 0.0, 0.06, and 0.09. (b) The same as Figure 3a but for an aerosol single scattering albedo of 0.95.

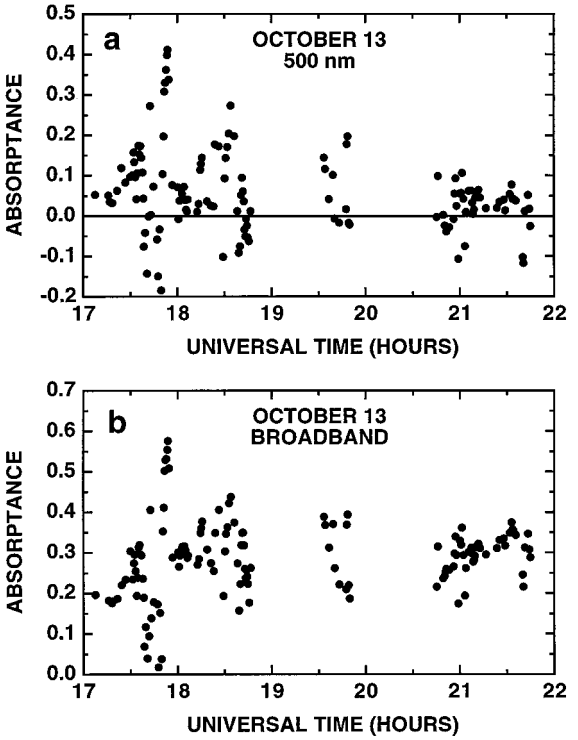

Figure 4. (a) The 500 nm column absorptance as a function of universal time for October 13. These are 30-s means. (b) The same as Figure 4a but for the broadband column absorptance.

Note that with clouds present, the 500 nm absorptances are as large as for clear conditions on October 11 (Figure 1), and this invariance to cloudiness is consistent with aerosol absorption. When the aerosol is imbedded within a cloud, two competing effects occur; aerosol absorption is increased because multiple scattering within the cloud increases the absorption path length, whereas it is reduced through reflection of SW radiation by the cloud, which reduces the amount of radiation that is available to be absorbed. The results shown in Figure 1 suggest these opposing effects are nearly compensatory, consistent with sensitivity studies we have performed using the radiative transfer model described by *Zender et al*. [1997]. The same argument would presumably also apply to a gaseous absorber. In the following section we utilize the 500 nm absorptance as a vehicle for studying sampling issues.

3. Sampling Issues

Sampling errors, which are not measurement errors but are caused by three-dimensional cloud effects associated with the measurement of column absorption by collocated aircraft, are demonstrated in Figure 4a (500 nm absorptance) and Figure 4b (broadband absorptance) for October 13, when broken cloud effects were very pronounced. These absorptances represent 30-s means. The first data gap corresponds to a refueling stop by the lower aircraft, while the second was caused by a telemetry failure that was subsequently corrected. As discussed

by *Valero et al*. [1997b], the flight began with a brief initial period of clear skies, followed by the presence of broken clouds, which resulted in the large positive and negative excursions to both absorptances shown in Figure 4. The upper aircraft was flying well above the cloud tops, while the lower aircraft was just below the cloud bottoms. When the lower aircraft was not in a cloud's shadow, but was receiving diffuse radiation coming from a cloud, there was an increase in the measured downward radiation, resulting in the downward absorptance spikes. The reverse occurs when the lower aircraft is below a cloud and thus is not measuring diffuse leakage of radiation from the sides of the cloud. Note the similar patterns in the positive-negative excursions for both the 500 nm and broadband absorptances.

Recently, *Marshak et al*. [1997] proposed a novel method for removal of the three-dimensional cloud effects (sampling errors) illustrated in Figure 4. With A denoting the measured broadband absorptance, they define a corrected absorptance as

$$A_{\text{cor}} = A - cA_0 \tag{1}$$

where A_0 denotes the absorptance in a spectral interval where there is no atmospheric (clear sky nor cloudy sky) absorption, and

$$c = dA/dA_0$$

as determined from a linear regression. As discussed by *Marshak et al*. [1997], (1) reduces to the *Ackerman and Cox* [1981] renormalization for $c = 1.0$, for which Ackerman and Cox assumed that wavelengths less than 700 nm characterized A_0. But as *Marshak et al*. [1997] demonstrate, through use of a Monte Carlo simulation with A_0 referring to a well-defined nonabsorbing spectral interval, the use of $c = 1.0$ overcompensates the removal of sampling errors and, consequently, $c < 1.0$. For present purposes, we adopt the following modification to (1):

$$A_{\text{cor}} = A - c(A_{500} - \bar{A}_{500}) \tag{2}$$

where A_{500} is the 500 nm absorptance and $\bar{A}_{500}$ is its flight-time-averaged mean value. The second term on the right side of (2) serves the same purpose as the comparable term in (1) but correcting for the fact that there is atmospheric absorption at 500 nm. It is important to recognize, as demonstrated in Figure 1, that A_{500} is invariant to the degree of cloudiness, thus making (2) comparable to (1); i.e., $(A_{500} - \bar{A}_{500})$ in (2) serves the same role as A_0 in (1). As appears in (2), $\bar{A}_{500}$ would be interpreted as the arithmetic mean of A_{500}. The proper definition of a mean absorptance, however, and denoted as $\langle A_{500} \rangle$, is that it is the ratio of the flight-time-averaged column absorption divided by the flight-time-averaged insolation at the upper aircraft; i.e., it is the ratio of averaged quantities rather than the average of a ratio. But this distinction is not important in the present application because $\bar{A}_{500} \approx \langle A_{500} \rangle$.

The slope determined from the linear regression in Figure 5a thus represents the value of c for use in (2), and the corrected broadband absorptance for October 13 is shown in Figure 5b. Note from Figure 5a that $c < 1.0$, consistent with *Marshak et al*. [1997]. That sampling errors have indeed been minimized is obvious when Figure 5b is compared to Figure 4b. Figures 6 and 7 provide the same information for October 30, when heavy overcast conditions prevailed, and the Figure 7b versus Figure 6b comparison again emphasizes the utility of this procedure. To demonstrate the importance of the sampling-error minimization when interpreting absorptance measurements, a scatterplot of the broadband absorptance as a function of the upper aircraft broadband albedo (the ratio of reflection to insolation measured at the upper aircraft) is shown in Figure 8a. This is similar to a plot introduced by *Arking* [1996] for interpreting satellite-surface measurements, although in his case, the slope was negative. The positive slope in Figure 8a is consistent with enhanced cloud absorption, as evidenced by the increasing absorptance with increasing upper aircraft albedo (i.e., increasing cloudiness), but the substantial scatter gives little confidence that this is meaningful, particularly in view of the cautionary comments regarding such plots by *Zhang et al*. [1997]. But this positive slope becomes much more meaningful when the corrected broadband absorptance is used (Figure 8b). In addition to the minimization of sampling errors through use of (2), such errors are reduced in the upper aircraft albedo because this aircraft was flying well above the clouds on October 13, and thus its downward facing instrument was spatially averaging the broken cloud fields [*Valero et al*., 1997b]. In some respects, October 13 was the most interesting of the 4 days, since it spanned the range from clear skies at the initiation of the flight to heavy overcast conditions later in the flight. Thus this single day provides the same information as the daily averages, for 4 days, shown in Figure 1; there is a significant increase in the broadband absorptance, in progressing from left to right, with increasing cloudiness. What is

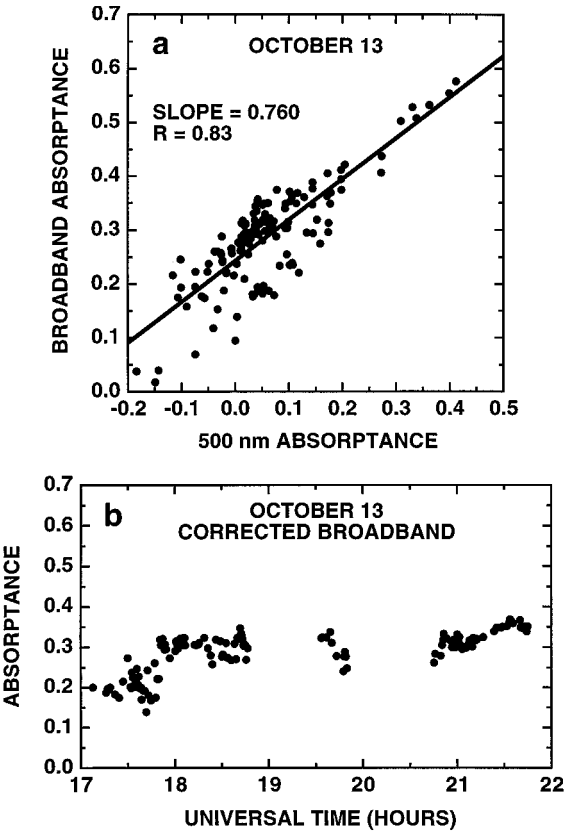

Figure 5. (a) The broadband absorptance as a function of the 500 nm absorptance for October 13. These are 30-s means. The straight line is a linear fit to the data. (b) The broadband absorptance for October 13, corrected using the procedure of *Marshak et al*. [1997], as a function of universal time. These are 30-s means.

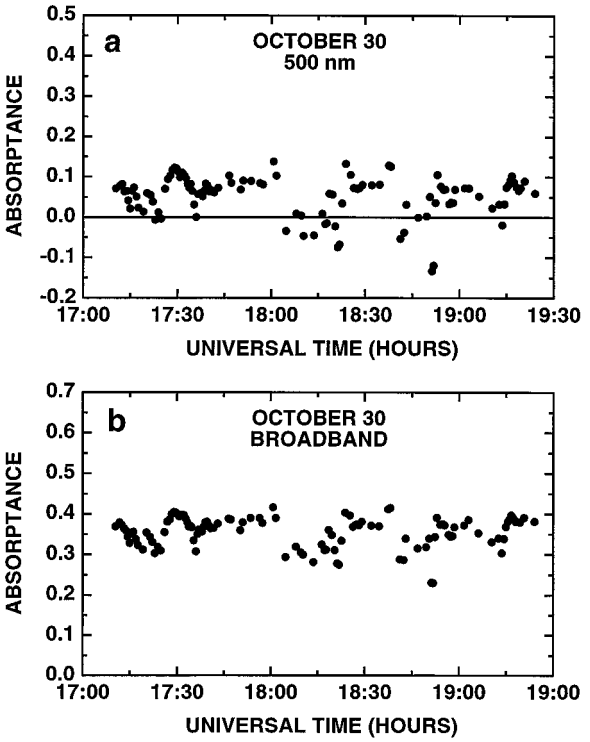

Figure 6. Same as Figure 4 but for October 30.

important in this Figure 1 versus Figure 8b agreement is that sampling errors have been removed in quite different ways. In Figure 1 they were removed through flight-time averaging that was of sufficient duration [*Valero et al*., 1997b], while in Figure 8b, which refers to much shorter timescales, sampling errors were minimized through use of the 500 nm measurements. This Figure 1 versus Figure 8b consistency gives us confidence that the observed cloud absorption is not an artifact of sampling errors. In addition, one would be hard pressed to ascribe the large absorptance on October 30 to sampling errors, given the minimal variability shown in Figure 7b. As in Figure 8b, a strong positive trend is found using a completely different suite of instruments, the near-infrared instruments that refer to the spectral interval from 680 to 3300 nm, and using (2) to correct the near-infrared column absorptance. This is shown in Figure 8c, where the absorptance and albedo both refer to the 680–3300 nm interval, which demonstrates there is substantial near-infrared enhanced cloud absorption.

There are difficulties, however, in combining the broadband and near-infrared measurements so as to partition the enhanced cloud absorption between wavelengths less than and greater than 680 nm, because this requires interfacing eight separate instruments. A potentially attractive approach is the regression shown in Figure 9a for October 13, where the modified near-infrared absorptance denotes the near-infrared column absorption divided by the upper aircraft broadband insolation. The attraction of this approach is that the regression slope should be invariant to instrument bias errors because such errors would not contribute to the trend. If the variability in this figure were caused solely by cloudiness variability, which is not the case as will be discussed shortly, then the regression slope would be unity if there were no cloud-induced absorption at wavelengths <680 nm because all cloud-induced absorption change would occur in the near infrared. Thus from the slope in Figure 9a, one might conclude that roughly 40% (0.58/1.58 $\approx$ 0.4) of the cloud-induced absorption occurs at wavelengths <680 nm. The problem with this interpretation is that the variability shown in Figure 9a is the combination of cloudiness variability and sampling errors, and the latter impact the slope differently than the former. This is demonstrated through use of the corrected absorptances shown in Figure 9b, which suggests that about 20% of the enhanced cloud absorption occurs at wavelengths <680 nm. And because the corrected absorptances might still contain residual sampling errors, this percentage is preferably stated as $\leq$20%.

4. Instrument Calibration Issues

The corrected broadband column absorption between the two aircraft, for October 13 and as a function of flight time, is illustrated in Figure 10a. The data in this plot have been normalized to the mean flight-time insolation measured at the upper aircraft so as to remove diurnal variations in column absorption caused by changes in solar zenith angle. This was accomplished through multiplying the corrected column absorptance (Figure 5b) by the flight-time-averaged upper aircraft insolation. Thus Figure 10a emphasizes the magnitude of the absorption variability in W m^{-2}, in contrast to the normalized absorption (absorptance) in Figure 5b. As discussed with reference to Figure 4, there was a brief initial period of clear skies, followed by broken clouds and periods when heavy overcast conditions prevailed. The point of Figure 10a is that, relative to the initial clear-sky absorption of roughly 150 W m^{-2}, there is a dramatic increase in column absorption when

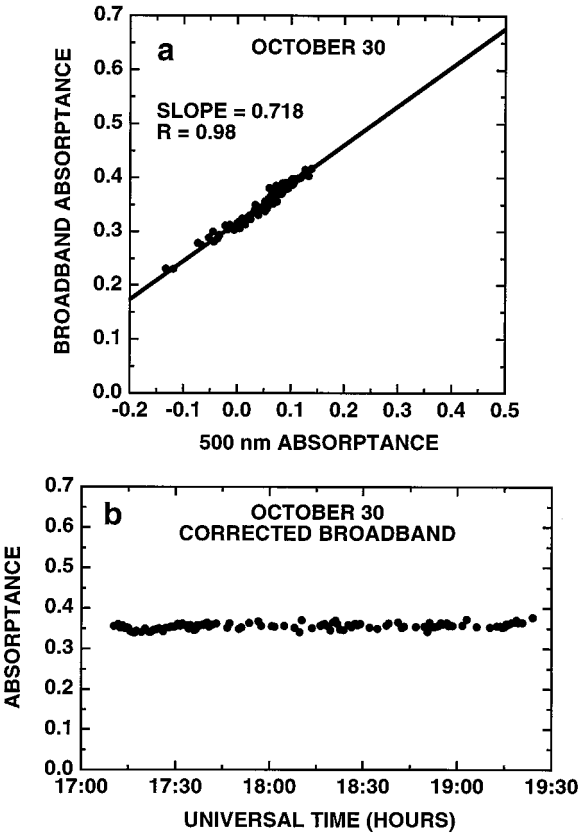

Figure 7. Same as Figure 5 but for October 30.

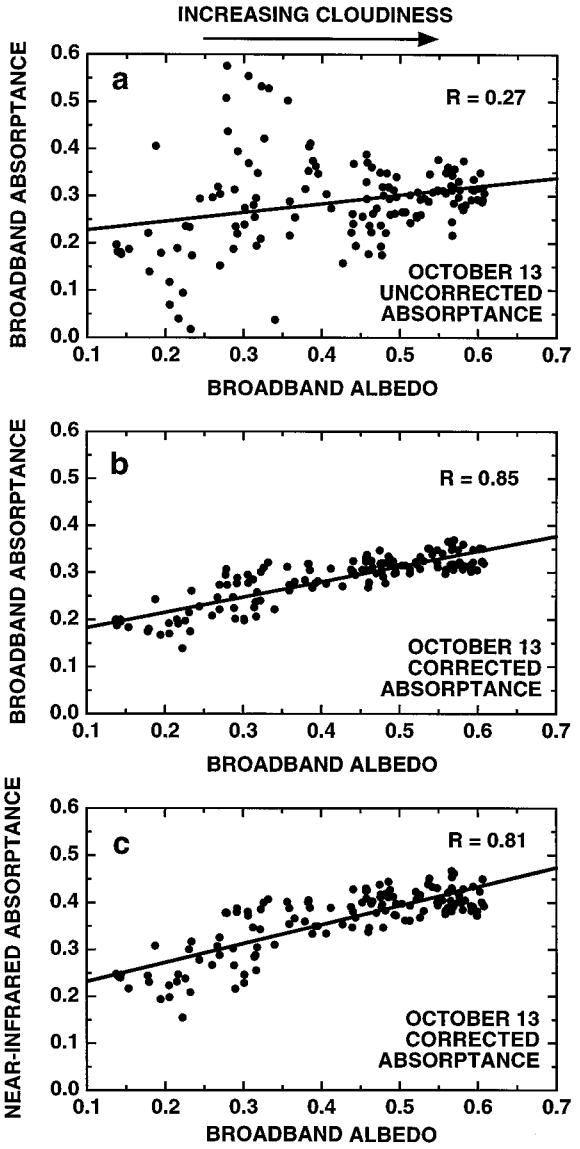

Figure 8. (a) The broadband absorptance as a function of the upper aircraft albedo for October 13. These are 30-s means, progressing from clear skies on the left to heavy overcast conditions on the right. The straight line is a linear fit to the data. (b) The same as Figure 8a but for the corrected absorptance. (c) The same as Figure 8a but for the corrected near-infrared absorptance as a function of the broadband albedo.

clouds are present, with one period when the absorption is roughly twice ($\approx$300 W m^{-2}) that for clear skies, consistent with Figure 1 when comparing the flight-time-averaged absorptance for October 30 (heavy overcast) to that for October 11 (clear). From the discussion of the previous section, it would be difficult to ascribe this 150 W m^{-2} cloud-induced absorption increase to sampling errors because these errors have already been minimized. And, as discussed below, it would be equally difficult to ascribe it to instrument calibration errors.

The SW column absorption in this experiment was derived using net fluxes measured at the upper aircraft and lower aircraft altitudes (14 km and 0.5–2 km, respectively). Most of the atmospheric absorption and any cloud absorption takes place between the two aircraft. So for any given absorption determination, radiative fluxes from four different radiometers must be combined. For the limit of thick clouds, however, it is obvious that one radiometer, the downward facing instrument on the upper aircraft, dominates the determination of column absorption. The upward facing radiometer on the upper aircraft measures something very close to the top-of-the-atmosphere (TOA) insolation, as illustrated in Figure 10b for October 13, the difference being consistent with atmospheric absorption and scattering processes above the upper aircraft. Any large error in this measurement would be easy to identify and certainly is not present. For large cloud optical depths, the lower aircraft measurements, made below the clouds, do not play a significant role in determining the column absorption. For the October 30 case the column transmittance is about 0.10 [*Valero et al.*, 1997b]. Thus, for example, a 10% error in the upward facing radiometer on the lower aircraft would give only a 0.01 error in the column absorptance (relative to the measured value of 0.36 in Figure 1). Therefore the large cloudy-sky column absorption, relative to clear skies, that we are observing is dominated by the downward facing instrument on the upper aircraft. If we hypothesize that this cloud absorption is caused by instrument error, then for the heavy-overcast conditions occurring near the end of the flight on October 13 (Figure 10a), the error in this instrument would have to be approximately -150 W m^{-2} to explain the roughly 150 W m^{-2} excess cloud absorption relative to the clear-sky initial portion of the flight. But if this were a bias error, then the measured clear-sky absorption during the initial flight portion would es-

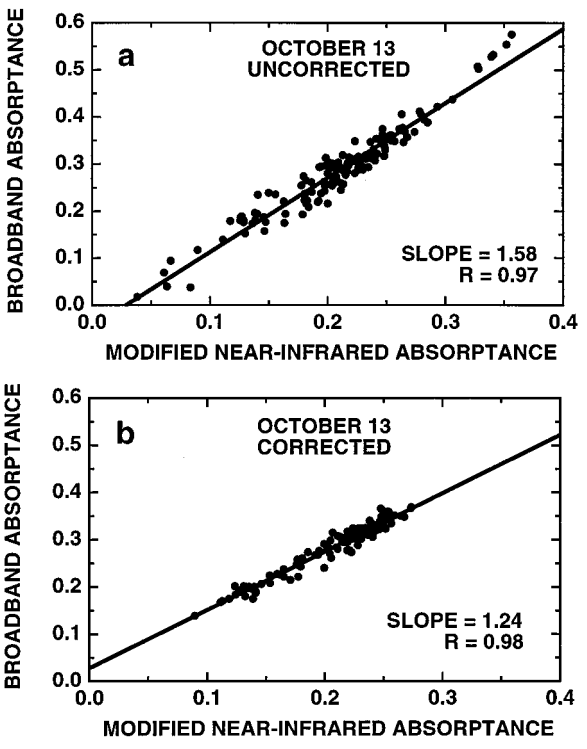

Figure 9. (a) The uncorrected broadband absorptance, for October 13, as a function of the uncorrected near-infrared absorptance which has been modified by normalizing it to the upper aircraft broadband insolation, in contrast to the near-infrared insolation. The straight line is a linear fit to the data. (b) The same as Figure 9a but using the corrected broadband and modified near-infrared absorptances.

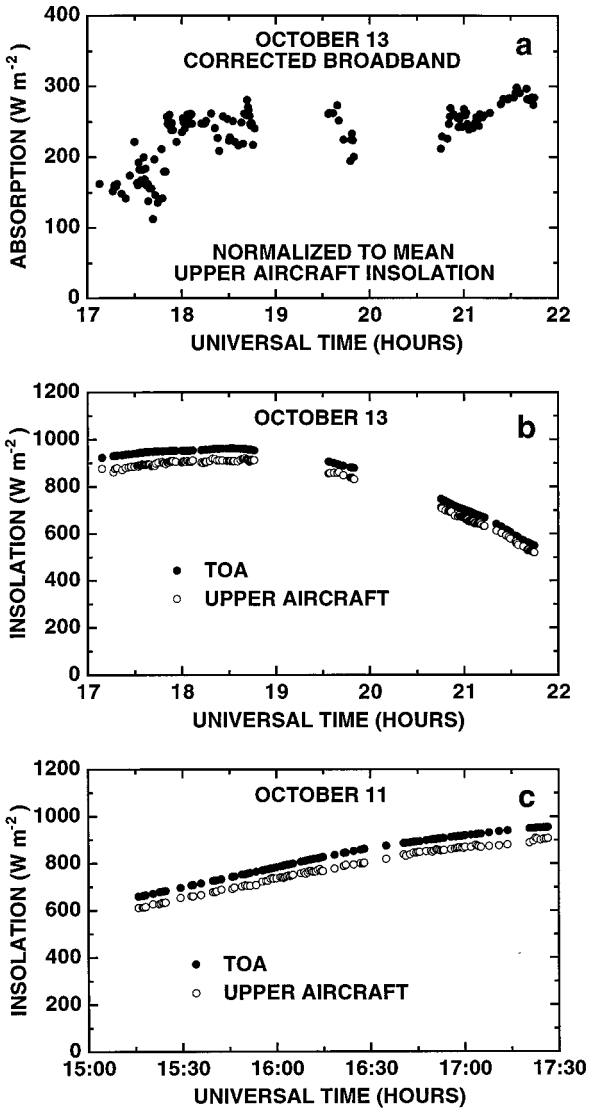

Figure 10. (a) The corrected column absorption, normalized to the mean upper aircraft insolation (see text), as a function of universal time for October 13. (b) Comparison of the measured upper aircraft insolation to the top-of-the-atmosphere (TOA) insolation, as a function of universal time, for October 13. (c) The same as Figure 10b but for October 11.

sentially be zero, in considerable conflict with theory. Nor is a gain error a plausible explanation, in which the instrument calibration might be reasonable for small signals (clear skies, dark underlying scene) but in error for large signals (heavy overcast, bright underlying scene). On October 13 the instruments on the upper aircraft were reversed, so that the downward facing instrument on October 13 was the upward facing instrument on October 11 when it was measuring a large and, relative to the TOA insolation, realistic signal as demonstrated in Figure 10c. Thus it is extremely unlikely that the substantial cloud absorption observed during part of the October 13 flight, and for all of the October 30 flight, is the artifact of an instrument calibration error. Nevertheless, the ARESE cases are only a few cloud cases, and additional field experiments are needed to confirm these results.

5. Conclusions

This investigation augments the conclusions made in the two prior ARESE studies [*Valero et al*., 1997b; *Zender et al*., 1997]. Specifically, it suggests that the rather large 500 nm column absorptance for clear skies (October 11, Figure 1) is caused by some temporally variable absorber, most likely aerosols. Likewise, aerosols are most plausibly the cause of the comparable 500 nm absorptances when clouds are present (Figure 1). Next, we have extended the prior investigation of sampling errors [*Valero et al*., 1997b] by employing the procedure of *Marshak et al*. [1997] to minimize sampling errors through use of the 500 nm measurements, and we conclude the enhanced cloud absorption is not likely an artifact of such errors, nor can it logically be explained by instrument calibration errors. We have empirically determined that at least some of the enhanced cloud absorption ($\leq$20%) occurs at wavelengths $<$680 nm, but the cause of this absorption, both at wavelengths $<$680 nm and in the near infrared, remains unknown; we find no evidence for its existence at 500 nm.

Acknowledgments. The authors gratefully acknowledge the many contributions that made ARESE possible. ARESE was conducted under the auspices of the Department of Energy's (DOE's) Atmospheric Radiation Measurements (ARM) Program and its Unmanned Aerospace Vehicle (ARM-UAV) component, with funding provided through the DOE's ARM Program, the Department of Defense's Strategic Environmental Research and Development Program (SERDP), and NASA's support of the ER-2. Numerous discussions among the ARESE, ARM, and ARM-UAV science teams helped shape the experiment and its subsequent analysis. A dedicated, multilaboratory field team spent more than 6 weeks in the field conducting the experiments on which this analysis is based. Without all these contributions, ARESE would not have been possible. We thank two anonymous referees for their helpful comments. This work was additionally supported by DOE through grant DEFG0395ER69183 to Scripps Institution of Oceanography, grants DEFG0285ER60314 and DEFG0290ER61063 to the State University of New York at Stony Brook, and grant DEFG0593ER61376 to the National Center for Atmospheric Research and by NASA through grant NAG53135 to the State University of New York at Stony Brook.

References

Ackerman, S. A., and S. K. Cox, Aircraft observations of shortwave fractional absorptance of non-homogeneous clouds, *J. Appl. Meteorol*., *20*, 1510–1515, 1981.

Arking, A., Absorption of solar energy in the atmosphere: Discrepancy between model and observations, *Science*, *273*, 779–782, 1996.

Barker, H. W., and Z. Li, Interpreting shortwave albedo-transmittance plots: True or apparent anomalous absorption?, *Geophys. Res. Lett*., *24*, 2023–2026, 1997.

Cess, R. D., et al., Absorption of solar radiation by clouds: Observations versus models, *Science*, *267*, 496–499, 1995.

Kato, S., T. P. Ackerman, E. E. Clothiaux, J. H. Mather, G. G. Mace, M. L. Wesely, F. Murcray, and J. Michalsky, Uncertainties in modeled and measured clear-sky surface shortwave irradiances, *J. Geophys. Res*., *102*, 25,881–25,898, 1997.

Marshak, M., A. Davis, W. Wiscombe, and R. Cahalan, Inhomogeneity effects on cloud shortwave absorption measurements: Two-aircraft simulations, *J. Geophys. Res*., *102*, 16,619–16,637, 1997.

Valero, F. P. J., A. Bucholtz, B. C. Bush, S. K. Pope, W. D. Collins, P. Flatau, A. Strawa, and W. J. Y. Gore, The Atmospheric Radiation Measurement Enhanced Shortwave Experiment (ARESE): Experimental and data details, *J. Geophys. Res*., *102*, 29,929–29,937, 1997a.

Valero, F. P. J., R. D. Cess, M. Zhang, S. K. Pope, A. Bucholtz, B. Bush, and J. Vitko Jr., Absorption of solar radiation by the cloudy atmosphere: Interpretations of collocated aircraft measurements, *J. Geophys. Res*., *102*, 29,917–29,927, 1997b.

Zender, C. S., S. Pope, B. Bush, A. Bucholtz, W. D. Collins, J. T. Kiehl,

F. P. J. Valero, and J. Vitko Jr., Atmospheric absorption during ARESE, *J. Geophys. Res*., *102*, 29,901–29,915, 1997.

Zhang, M. H., R. D. Cess, and X. Jing, Concerning the interpretation of enhanced cloud shortwave absorption using monthly mean Earth Radiation Budget Experiment/Global Energy Balance Archive measurements, *J. Geophys. Res*., *102*, 25,899–25,905, 1997.

R. D. Cess and M. Zhang, Marine Sciences Research Center, State University of New York, Stony Brook, NY 11794-5000. (cess@atmsci.msrc.sunyb.edu)

A. Bucholtz, B. Bush, S. K. Pope, and F. P. J. Valero, Scripps Institution of Oceanography, University of California at San Diego, La Jolla, CA 92093-0242.

C. S. Zender, National Center for Atmospheric Research, Boulder, CO 80307-3000.

J. Vitko Jr., Sandia National Laboratory, P. O. Box 969, MS 9056, Livermore, CA 94550.

(Received March 17, 1998; revised August 24, 1998; accepted October 20, 1998.)